© 2021. Published by The Company of Biologists Ltd | Journal of Experimental Biology (2021) 224, jeb232074. doi:10.1242/jeb.232074

RESEARCH ARTICLE

Ciliary Ca^{2+} pumps regulate intraciliary Ca^{2+} from the action potential and may co-localize with ciliary voltage-gated Ca^{2+} channels

Junji Yano*, Russell Wells, Ying-Wai Lam and Judith L. Van Houten

ABSTRACT

Calcium ions (Ca^{2+}) entering cilia through the ciliary voltage-gated calcium channels (Ca_V) during the action potential causes reversal of the ciliary power stroke and backward swimming in *Paramecium tetraurelia*. How calcium is returned to the resting level is not yet clear. Our focus is on calcium pumps as a possible mechanism. There are 23 *P. tetraurelia* genes for calcium pumps that are members of the family of plasma membrane Ca^{2+} ATPases (PMCAs). They have domains homologous to those found in mammalian PMCAs. Of the 13 pump proteins previously identified in cilia, ptPMCA2a and ptPMCA2b are most abundant in the cilia. We used RNAi to examine which PMCA might be involved in regulating intraciliary Ca^{2+} after the action potential. RNAi for only *ptPMCA2a* and *ptPMCA2b* causes cells to significantly prolong their backward swimming, which indicates that Ca^{2+} extrusion in the cilia is impaired when these PMCAs are depleted. We used immunoprecipitations (IP) to find that ptPMCA2a and ptPMCA2b are co-immunoprecipitated with the Ca_V channel α1 subunits that are found only in the cilia. We used iodixanol (OptiPrep) density gradients to show that ptPMCA2a and ptPMCA2b and Ca_V1c are found in the same density fractions. These results suggest that ptPMCA2a and ptPMCA2b are located in the proximity of ciliary Ca_V channels.

KEY WORDS: Calcium signaling complex, Cilia, Detergent-resistant membranes, *Paramecium*, Plasma membrane Ca^{2+}-ATPase, Voltage-gated Ca^{2+} channel

INTRODUCTION

The plasma membrane Ca^{2+}-ATPases (PMCAs) play important roles in the regulation of intracellular Ca^{2+} concentrations (Calì et al., 2017; Strehler, 2015). The PMCAs, the sarco- and endoplasmic reticulum Ca^{2+}-ATPase (SERCA) and the Na^+–Ca^{2+} exchanger (NCX) all have different kinetic properties and roles in calcium homeostasis and regulation (Blaustein and Lederer, 1999; Brini and Carafoli, 2011; Saidu et al., 2009; Vandecaetsbeek et al., 2011). In contrast to NCX and SERCA, the PMCAs are generally thought to be low-capacity and high-affinity transporters that can bring Ca^{2+} levels to very low resting levels (Brini and Carafoli, 2011; Carafoli, 1994). Although mammals encode only four PMCA genes, they have a variety of pumps with different characteristics due to additional variants (isoforms) created by alternative splicing at two sites (Di Leva et al., 2008; Strehler and Zacharias, 2001). The isoforms show differences in regulation by Ca^{2+}/calmodulin, protein kinase A, protein kinase C and acidic phospholipids. Isoforms can differ in basal activity in the absence of calmodulin, rates of activity in the presence of Ca^{2+}/calmodulin, and rates of inactivation by calmodulin (Calì et al., 2017; Di Leva et al., 2008; Strehler and Zacharias, 2001). In addition, mammalian PMCA activity can be modulated by formation of protein complexes and localization in specialized domains (e.g. lipid rafts) of the plasma membrane (Lopreiato et al., 2014; Padányi et al., 2016; Strehler, 2015). These domains are considered to be liquid-ordered (Brown, 2006) that organize biological membranes into regions with specific protein compositions and functions (Levental et al., 2020). The domains are dynamic and provide a favorable environment for the protein–protein interactions needed for signal transduction (Simons and Toomre, 2000). As it is difficult to image or otherwise demonstrate lipid rafts, we turned to biochemical methods to isolate and analyse membrane fractions. Cell membranes are not fully solubilized in non-ionic detergents, leaving behind components called detergent-resistant membranes (DRMs) that can be isolated on density gradients along with most of the proteins generally targeted to rafts (Brown, 2006; Levental et al., 2020). Therefore, we refer to the density fractions of ciliary membranes in our analysis of *Paramecium* as DRMs.

In *Paramecium* cells, the frequency and direction of ciliary beating are controlled by membrane potential and intraciliary Ca^{2+} (Eckert, 1972; Kung et al., 1975; Machemer, 1988). When the cells are depolarized sufficiently to trigger an action potential, there is an influx of calcium into the cilia through voltage-gated calcium (Ca_V) channels. This increased Ca^{2+} at the ciliary axoneme changes the power stroke, and causes the cell to swim backwards. The Ca_V channels responsible for the action potential are found only in the cilia (Dunlap, 1977; Lodh et al., 2016). Free intraciliary Ca^{2+} is estimated to rise from low levels (100 nmol l^{-1}) to 10 µmol l^{-1} to 1 mmol l^{-1} during the action potential (Eckert, 1972; Husser et al., 2004; Oertel et al., 1977). The Ca^{2+} entering through the ciliary Ca_V channel does not spill into the cytoplasm (Husser et al., 2004).

The resting membrane potential is restored after the action potential by voltage-gated potassium (K_V) channels and calcium activated potassium (K_{Ca}) channels (Brehm et al., 1978; Oertel et al., 1977; Satow and Kung, 1980). However, the mechanism that returns the intraciliary calcium to 100 nmol l^{-1} or less for the cells to resume forward swimming is not clear. It has been hypothesized that calcium ATPase or PMCA accomplish this removal of Ca^{2+} after the action potential (Doughty and Dryl, 1981; Eckert and Brehm, 1979). Because there remain sceptics about this role of PMCAs (Plattner, 2015), and the specific isoforms that might participate in removing ciliary Ca^{2+} are not known, we changed from our previous biochemical characterizations of PMCAs to molecular approaches in order to provide clear evidence for or against the participation of PMCAs in ciliary Ca^{2+} removal.

Department of Biology, University of Vermont, Burlington, VT 05405, USA.

*Author for correspondence (Junji.Yano@uvm.edu)

J.Y., 0000-0001-6600-3624

Received 26 June 2020; Accepted 2 March 2021

Journal of Experimental Biology (2021) 224, jeb232074. doi:10.1242/jeb.232074

The first plasma membrane Ca^{2+}-ATPase gene (*AAB81284*) in *P. tetraurelia* was cloned using inverse PCR with degenerate primers deduced from homologous amino acid sequences among various PMCAs (Elwess and Van Houten, 1997). The amino acid sequence identified has the same molecular characteristics as mammalian PMCAs, such as conserved domains for an acylphosphate intermediate, an ATP-binding site, a hinge, a calcium transport site and a calmodulin binding domain at the C-terminus (Van Houten, 1998). We further annotated 23 putative *ptPMCA* genes (presented here, see Table 1) using *P. tetraurelia* genome databases provided by Genoscope (https://www.genoscope.cns.fr). Our proteomics study of ciliary membranes identified 13 PMCA proteins (Yano et al., 2013). Proteomic studies of cilia and the ciliary membrane in *P. tetraurelia* by our group and Sperling's group showed that of the 13 proteins, two almost identical isoforms (paralogs), ptPMCA2a and ptPMCA2b, are enriched in the cilia (Arnaiz and Sperling, 2011; Lodh, 2012; Yano et al., 2013, 2015).

We narrowed down the search for the PMCAs that might participate in removal of ciliary Ca^{2+} from the action potential by using RNA interference (RNAi) for the 13 PMCAs identified by proteomic analysis of the ciliary membrane and assaying for prolonged backward swimming as the read-out for sustained raised intraciliary Ca^{2+}. We found that RNAi for only *ptPMCA2a* and *ptPMCA2b* elicits very long backward swimming. The cells lengthened their backward swimming duration under the depolarization, which suggested that, without these pumps, intraciliary Ca^{2+} remains high after the action potential and sustains backward swimming long after it should stop.

Previously, we identified Ca_V channels α1 subunits (Ca_V1a, Ca_V1b and Ca_V1c) that were located only in cilia as expected for the channels responsible for the action potential (Lodh et al., 2016; Valentine et al., 2012). In the present work, we found that ptPMCA2a and ptPMCA2b and the Ca_V channel α1 subunits could be co-immunoprecipitated (co-IP) from the ciliary membrane. The PMCAs and these Ca_V channels were also found in the same ciliary membrane fractions in iodixanol (OptiPrep) density gradients of DRMs.

MATERIALS AND METHODS

Cell lines and culture

Paramecium tetraurelia 51s (sensitive to killer) cells were cultured in a wheat infusion medium inoculated with *Aerobacter aerogenes* at 22°C (Sasner and Van Houten, 1989). All reagents, except for those specified by the company name, were purchased from Sigma-Aldrich (St Louis, MO, USA). Milli-Q ultrapure water (Millipore/Sigma-Aldrich) was used for all molecular and biochemical experiments.

Plasma membrane calcium ATPases in *P. tetraurelia* (ptPMCA)

Using the PMCA gene that we cloned previously (Elwess and Van Houten, 1997), we identified and annotated 23 putative PMCA genes among macronuclear genome sequences of *P. tetraurelia*, strain d2-4, provided by Genoscope (www.genoscope.cns.fr) and deposited to EMBL through Genoscope (Table 1). The phylogeny.fr database (www.phylogeny.fr/) was used for the phylogenetic analysis of macronuclear DNA or amino acid sequences.

RNAi plasmid construction

The genes coding for the 13 PMCA proteins that were detected in our proteomics study of the ciliary membrane (Yano et al., 2013) were used for RNAi experiments (*ptPMCA1a*, *-1b*, *-1c*, *-2a*, *-2b*, *-3a*, *-3b*, *-4a*, *-4b*, *-7a*, *-7b*, *-8a* and *-8b*). PCR primers used for amplifying *PMCA* genes are shown in Table S1. PCR products were ligated into the L4440 plasmid (Lodh et al., 2016). All selected gene segments that we designed for RNAi, except for *ptPMCA3a* and *ptPMCA3b*, are unique with no predicted RNAi off-target effects from stretches of 23 nucleotides as tested using the off-target tool (Li and Durbin, 2009) on ParameciumDB (Arnaiz and Sperling, 2011). A unique sequence of length suitable for RNAi (more than 200 bases) was not found to distinguish between *ptPMCA3a* and *ptPMCA3b*. Instead, the sequence region of *ptPMCA3a* with high identity to *ptPMCA3b* was selected (Table S1). The forward and reverse primers were designed to amplify sequences of both

Table 1. Plasma membrane calcium ATPase (*ptPMCA*) genes and new nomenclature in *Paramecium tetraurelia*

GenBank	Gene name, old	Gene name, new	Open reading frame (ORF) (bp)	Intron	Length (amino acids)	Molecular mass (kDa)	Scaffold
CR932147	*PMCA2*	*ptPMCA1a*	3441	4	1146	129.40	12
CR932150	*PMCA3*	*ptPMCA1b*	3372	3	1123	126.00	101
CR933346	*PMCA4*	*ptPMCA1c*	3372	3	1123	125.88	46
CR933342	*PMCA18*	*ptPMCA2a*	3543	8	1180	131.45	52
CR932132	*PMCA19*	*ptPMCA2b*	3519	8	1172	130.70	60
CR932141	*PMCA13*	*ptPMCA3a*	3247	4	1148	128.32	23
CR932139	*PMCA16*	*ptPMCA3b*	3444	4	1147	127.79	87
CR932133	*PMCA14*	*ptPMCA4a*	3381	5	1126	125.98	79
CR933344	*PMCA15*	*ptPMCA4b*	3381	5	1126	125.77	64
CR932135	*PMCA23*	*ptPMCA4c*	3354	4	1117	126.68	76
CR933343	*PMCA24*	*ptPMCA4d*	3387	4	1128	127.54	67
CR932145	*PMCA5*	*ptPMCA5a*	3153	3	1050	117.41	137
CR933349	*PMCA12*	*ptPMCA5b*	3129	4	1042	116.29	27
CR933347	*PMCA6*	*ptPMCA6a*	3204	4	1067	119.80	72
CR933348	*PMCA10*	*ptPMCA6b*	3225	4	1074	119.47	54
CR932152	*PMCA11*	*ptPMCA6c*	3210	4	1069	119.30	135
CR932151	*PMCA7*	*ptPMCA7a*	3204	5	1067	118.91	18
CR933345	*PMCA21*	*ptPMCA7b*	3201	5	1066	118.86	44
CR932144	*PMCA8*	*ptPMCA8a*	3204	6	1067	118.65	144
CR932153	*PMCA9*	*ptPMCA8b*	3204	6	1067	119.03	123
CR932137	*PMCA17*	*ptPMCA9a*	3398	8	1065	118.71	3
CR932134	*PMCA20*	*ptPMCA9b*	3398	8	1065	118.87	6
CR932143	*PMCA22*	*ptPMCA9c*	3207	8	1068	119.71	7

Journal of Experimental Biology (2021) 224, jeb232074. doi:10.1242/jeb.232074

ptPMCA3a and *ptPMCA3b*, meaning that both genes were purposely silenced concurrently with RNAi. For other genes, while we selected sequences that had no predicted off-target effects, we found nonetheless that mRNA for paralogs was often decreased along with the intended paralog's mRNA. This is probably due to secondary siRNAs as predicted by Carradec et al. (2015). Therefore, we examined the effects of RNAi for each set of paralogs using RT-PCR to understand the specificity or lack thereof for the gene silencing.

Feeding RNAi

The HT115 bacteria transfected with plasmid L4440 without insert (empty vector for control) or with insert were added to the culture fluid for *Paramecium* cells, following the published protocol (Lodh et al., 2016; Valentine et al., 2012). When more than one gene was to be silenced, a mixture of bacteria was fed to the cells (Lodh et al., 2016; Nabi et al., 2019). The paramecia were cultured at 22°C. Around 72 h after the start of feeding RNAi, cell behavior was examined under depolarizing conditions and total RNA was isolated for reverse transcription polymerase chain reaction (RT-PCR).

RT-PCR

Total RNA was isolated using E.Z.N.A.® HP Total RNA kit (Omega Bio-Tek, Norcross, GA, USA). The first strand cDNA was synthesized using 1 µg total RNA, poly dT 20 primer and SuperScript® III reverse transcriptase (Thermo Fisher Scientific, Waltham, MA, USA), following the protocol provided by the company. A dilution series of first strand cDNA was diluted 1:10, 1:100 and 1:1000 in order to better visualize differences in RT-PCR. PCR was carried out in 30 cycles with denaturation at 95°C for 30 s, annealing at 45°C for 1 min and extension at 68°C for 1 min for calmodulin primers, and with denaturation at 95°C for 30 s, annealing at 55°C for 1 min and extension at 68°C for 1 min for PMCA primers. PCR products were separated on 1.5% agarose gels and stained with ethidium bromide. The intensities of bands for calmodulin control and a PMCA were compared across their dilution series.

Behavior assay

The following solutions were used for assays of backward swimming duration: 4 mmol l^{-1} KCl in the basic buffer of 1 mmol l^{-1} calcium citrate and 1 mmol l^{-1} Tris, adjusted to pH 7.0 with Tris (Lodh et al., 2016) was used as the resting solution; 30 mmol l^{-1} KCl, 1 mmol l^{-1} $BaCl_2$, 20 mmol l^{-1} NaCl or 20 mmol l^{-1} NaCl/10 mmol l^{-1} TEA-Cl in the same basic buffer was used for test solution. TEA-Cl is tetraethyl ammonium chloride, which inhibits voltage-gated K^+ (K_V) channels. By using TEA to inhibit K_V, we can focus on the Ca^{2+}-activated K^+ (K_{Ca}) channels, which are left to repolarize the cell after the action potential (Brehm et al., 1978; Oertel et al., 1977; Satow and Kung, 1980). Note that all buffers were not made by adding salts to the resting solution; rather, each was made separately and pH was adjusted at the end before adjusting the volume. The cells were kept in the resting solution for 20 min, and then transferred one by one to a depression slide filled with the testing solution under a stereomicroscope using a micropipette. The backward swimming duration was measured from the start of backward movement to the onset of whirling in place because, after whirling, cells change direction and start to swim forward. The assay was carried out at 22°C. Temperature control was critical. A two-tailed Mann–Whitney *U*-test was used for statistical analysis because in our experience with behavioral data, we cannot assume a normal distribution.

Microinjection and culture for injected cells

We injected 5 µg µl^{-1} of the expression plasmid (pPXV-FLAG-*Ca_V1a*, *-1b*, *-1c* or pPXV-FLAG) into the macronucleus of individual *Paramecium* cells. The injected cells were individually cultured and each established as a cell line. The selection of transformed cell lines was carried out following previous methods (Yano et al., 2003). The cell lines with the highest copy number were maintained at 15°C by transferring five cells to fresh culture fluid every week. For immunoprecipitation (IP) and OptiPrep density experiments, cells were cultured in the richer wheat culture fluid (Wright and Van Houten, 1990) of 3–6 liters at 22°C.

2aN polyclonal antibody (2aN pAb)

This polyclonal antibody (pAb) was produced in a rabbit against a synthetic peptide (2aN) of FKSGLTMNDQSERERAFGHN corresponding to 66th to 85th amino acids in the N-terminus of ptPMCA2a, and affinity-purified by GenScript (Piscataway, NJ, USA). The purified antibody was named 2aN pAb.

Previously we showed that the 2aN antibody when pre-absorbed with the 2aN peptide no longer recognized GST-2aN on blots, compared with mock pre-absorbed antibody that did recognize GST-2aN (M. Valentine and J.Y., unpublished observation). In this study, we show by liquid chromatography-tandem mass spectrophotometry (LC-MS/MS) that proteins of about 130 kDa (the approximate mass of the ptPMCAs) identified by the 2aN antibody comprised ptPMCA2a and ptPMCA2b with a small contribution of ptPMCA3 and ptPMCA4 (see Table S3b).

Immunoprecipitation and co-IP

The ciliary isolation, IP and co-IP were carried out following previous methods (Lodh et al., 2016; Yano et al., 2013). Cilia from cells expressing FLAG-Ca_V1a, FLAG-Ca_V1b, FLAG-Ca_V1c or only FLAG were solubilized with 1% Triton X-114 in membrane buffer (10 mmol l^{-1} Tris buffer, pH 7.4, 50 mmol l^{-1} KCl, 5 mmol l^{-1} $MgCl_2$, 1 mmol l^{-1} EGTA) or FLAP200 (50 mmol l^{-1} Hepes, 200 mmol l^{-1} KCl, 1 mmol l^{-1} EGTA, 1 mmol l^{-1} $MgCl_2$, pH 7.8) at 4°C for 1 h and then centrifuged at 14,000 ***g*** for 10 min at 4°C. Free Ca^{2+} was 3.1×10^{-11} mol l^{-1} in the membrane buffer, and 2.3×10^{-11} mol l^{-1} in FLAP200 (https://somapp.ucdmc.ucdavis.edu/pharmacology/bers/maxchelator/CaEGTA-TS.htm) or less than 1 nmol. The supernatant was used for IP. We used Triton X-114 for solubilization because we found that this detergent solubilizes integral hydrophobic ciliary membrane proteins very well (Yano et al., 2013). See Lodh et al. (2016) for the flow charts for solubilization, the use of Triton X-114, and the generation of the supernatants used for IP.

Anti-FLAG M2 affinity gel (30 µl) was used for IP of FLAG-Ca_V1s or FLAG, and 2aN antibody (15 µg) for IP of ptPMCA2a. Anti-glutathione-*S*-transferase (GST, 15 µg) was used for a control IP. Protein A beads (Amersham Pharmacia/GE HealthCare, Chicago, IL, USA) (20 µl) were used for IP of 2aN and anti-GST antibodies. After IP, anti-FLAG M2 gel and Protein A beads were mixed with 50 µl membrane buffer for sodium dodecyl sulfate-polyacrylamide gel electrophoresis (SDS-PAGE).

OptiPrep analysis of detergent-resistant membranes

We used cold non-ionic detergent Triton X-100 to isolate DRMs (Simons and Toomre, 2000; Nebl et al., 2002; Brown, 2006). The detergent-insoluble pellets were subsequently separated on density gradients (Brown, 2006; Kenworthy, 2020; Simons and Toomre, 2000). We used fractionation by density (below) to investigate which proteins from the DRMs share the same biochemical density separation properties.

About 8 mg of cilia isolated following a previous protocol (Yano et al., 2013) were solubilized with solubilization buffer [1% Triton X-100 in 150 mmol l^{-1} NaCl, 5 mmol l^{-1} dithiothreitol (DTT), 5 mmol l^{-1} EDTA and 25 mmol l^{-1} Tris; pH 7.4] containing protease inhibitors [100 µmol l^{-1} phenylmethlsulfonyl fluoride, 1 µg ml^{-1} Leupepsin (Research Products International, Mount Prospect, IL, USA) and 1 µg ml^{-1} Pepstatin (Research Products International)] for 1 h at 4°C. After centrifuging at 48,400 ***g*** at 4°C for 30 min, the pellet (DRM) was completely re-suspended with the solubilization buffer for at 4°C for 15 min, and then mixed with 60% iodixanol (OptiPrep) at a final concentration of 40%. The mixture was placed on the bottom of an ultra-centrifuge tube (Beckman Coulter Life Science, Indianapolis, IN, USA). Aliquots of 650 µl each of 35, 30, 25, 20 and 0% OptiPrep prepared in the solubilization buffer were loaded from the bottom in order. For floating the membranes, the centrifuge tubes were placed in a Beckman SW 60 Ti swinging bucket rotor and centrifuged at 160,000 ***g*** at 4°C for 4 h in Beckman LB-70M ultracentrifuge. Eight fractions each with equal volumes of 500 µl were harvested from top to bottom in each tube. These fractions were each mixed with the solubilization buffer and then centrifuged at 48,400 ***g*** at 4°C for 30 min. The pellets were re-suspended and volume adjusted to 50 µl membrane buffer each for PAGE. The protease inhibitors mentioned above were included in all procedures.

Western blot analysis

Fifty microliters of 2×SDS sample buffer (120 mmol l^{-1} Tris-HCl, pH 6.8, 4% SDS, 20% glycerol and 0.02% w/v Bromophenol Blue) were added to the samples of 50 µl from IP or OptiPrep. The proteins precipitated with IP and the proteins fractionated by OptiPrep were separated on 4–18% SDS-PAGE and analysed on western blots, following the published protocols (Lodh et al., 2016; Yano et al., 2013). The antibodies used for western blot analysis of IP, co-IP and OptiPrep proteins were: FLAG pAb (F3165-5MG, dilution to 1:2500), FLAG monoclonal antibody (mAb) (F7425-0.2MG, 1:5000), anti-2aN pAb (1:2500), α-tubulin mAb (T6199, 1:10,000), GST pAb (GE27-4577-01, 1:5000) and surface antigen 51B (sAG_51B) pAb (1:5000, gift from Drs J. Forney and M. Simon).

Silver-stained gels

Of the samples obtained from IP or OptiPrep, 20% of each was used for western blots and the rest for silver-stained gels. Molecular mass markers were included in the electrophoresis. In IP cases, the gel was cut in two parts, one for western blot and another for silver stain; fragments of the molecular mass markers can be seen. The silver stain was carried out following the previous protocol (Lodh et al., 2016; Yano et al., 2013). The silver-stained gel bands matching the band detected by a particular antibody on the western blot were cut out from the control and test IP lanes, or the lanes with OptiPrep™ prepared samples for the mass spectrometry (MS) analysis.

Protein identification by liquid chromatography-tandem mass spectrometry

LC-MS/MS analyses were performed following published protocols with some modifications (Lodh et al., 2016; Yano et al., 2013). In-gel trypsin digestion was carried out at a final concentration of 6 ng ml^{-1} trypsin (Promega, Madison, WI, USA) in 5% CH_3CN and 40 mmol l^{-1} NH_4HCO_3 at 37°C for no more than 18 h. The digested peptides were sequentially extracted with 5% formic acid (FA) and 50% acetonitrile, and 100% acetonitrile, and then dried. The dried peptides were re-suspended in 10 µl of a solution of 2.5% CH_3CN and 2.5% FA, and then 5 µl of the resuspension was analysed on the linear ion trap (LTQ XL) mass spectrometer (Thermo Fisher Scientific). Peptides were loaded onto a 100 µm inner diameter capillary fused silica column packed with MAGIC C18 (5 µm particle size, 20 nm pore size, Michrom BioResources, Auburn, CA, USA) at a flow rate of 500 nl min^{-1} and were separated by a gradient of 2.5–35% CH_3CN/0.1% FA, 35–100% CH_3CN/0.1% FA and 100% CH_3CN/0.1% FA, followed by an immediate return to 2.5% CH_3CN/0.1% FA and a hold at 2.5% CH_3CN/0.1% FA. Peptides were introduced into the mass spectrometer via a nanospray ionization source and a laser pulled ∼3 µm orifice at a spray voltage of 1.8 kV. MS data were acquired in a data-dependent 'top 10' acquisition mode, in which a survey scan from *m/z* 400–1600 was followed by 10 collision-induced dissociation (CID) tandem mass spectrometry (MS/MS) scans of the most abundant ions. MS/MS scans were acquired with the following parameters: isolation width: 2 *m/z*, normalized collision energy: 35%, activation Q: 0.250 and activation time: 30 ms, and dynamic exclusion enabled. Product ion spectra were searched with SEQUEST using Proteome Discoverer 2.4 (Thermo Fisher Scientific) against the *Paramecium* database (http://paramecium.i2bc.paris-saclay.fr/; Arnaiz et al., 2020) in a concatenated target–decoy fashion. Search parameters were as follows: (1) full trypsin enzymatic activity, (2) maximum missed cleavages=2, (3) minimum peptides length=6, (4) mass tolerance of 2 Da for precursor ions and 0.8 Da for fragment ions, (5) dynamic modifications on methionine (+15.9949 Da: oxidation) and (6) four maximum dynamic modifications allowed per peptide. Percolator node was included in the workflow to limit the false positive (FP) rates to less than 1% in the dataset.

All the raw files of the gel bands derived from each sample lane were searched against the database as one contiguous input file, resulting in one result file (.msf) for each sample (e.g. CONTROL, TEST). Multiple gel bands were cut out from the same lane (from the same sample). The digest from each band was analysed individually by mass spectrometry. As these bands belonged to the same sample, the raw data generated for individual bands were imported into the software as 'fractions'. The raw files were thus combined before analysing, resulting in one .msf result file for each sample. The .msf files were incorporated into Scaffold 4.11 (Proteome Software, Portland, OR, USA) as mudPIT with 'prefiltered mode' and protein cluster analysis to compare the unique peptide counts between 'CONTROL' and 'TEST' with respect to specific protein isoforms. False discovery rate (FDR) at protein and peptide levels at 1% and 'Minimum number of peptides'=1 were selected to achieve less than 1% protein and peptide decoy FDR in the filtered dataset. Peptide identifications were shown with the corresponding XCorr values listed in Table S3. If two or more peptides matched to a certain protein, the protein was considered to be identified and shown in Table S3.

Other analyses (not included in Table S3) were run on the Q Exactive mass spectrometer coupled to an EASY-nLC system (Thermo Fisher Scientific) and analysed by Proteome Discoverer with appropriate instrument settings and parameters for searches (Nabi et al., 2019). For these samples, cysteine reduction and alkylation were performed before in-gel digestion as follows: after destaining the silver-stained gel pieces, disulfide bonds were reduced with 10 mmol l^{-1} DTT in 100 mmol l^{-1} NH_4HCO_3 for 1 h at 56°C. After discarding the DTT solution, cysteines were alkylated with 10 mg ml^{-1} iodoacetamide (IAA) in 100 mmol l^{-1} NH_4HCO_3 for 40 min in the dark at room temperature. After discarding the IAA solution, the gel pieces were washed in 100 mmol l^{-1}

Journal of Experimental Biology (2021) 224, jeb232074. doi:10.1242/jeb.232074

NH_4HCO_3 and then dehydrated in 100% acetonitrile twice. Static modification on cysteine (+57.0215 Da: carbamidomethylation) was added as a search parameter.

RESULTS

Plasma membrane calcium ATPases in *P. tetraurelia* (ptPMCA)

We identified and annotated 23 putative *ptPMCA* genes using macronuclear genomic DNA sequences of *P. tetraurelia* d4-2 provided by Genoscope. See Table 1 for accession numbers and gene names.

Figure 1 shows the phylogenetic relationships among the 23 *ptPMCA* genes, which fall into nine paralog groups (*ptPMCA1–9*) resulting from three whole genome duplications (WGD) (Aury et al., 2006). In Table 1, we organized the 23 *ptPMCA* gene names according to paralog groups. We propose that *ptPMCA* gene names should be revised in ParameciumDB following the concept of paralogs (Arnaiz and Sperling, 2011). See Table 1 where we provide both our new nomenclature and that of ParameciumDB. At the amino acid sequence level, the members within each paralog group are between 56 and 97% identical. The paralogs *ptPMCA4c* and *ptPMCA4d* show the lowest identity of 56%. The identities among the nine paralog groups are between 31 and 80%. The 13 ciliary PMCAs identified in a previous proteomic study are shown in red (Yano et al., 2013). There is nothing in the gene sequences coding for ciliary *ptPMCAs* that would distinguish them among the 23 for their location in the cilia.

When compared with human sequences, all *Paramecium* ptPMCAs have 35–42% identity with human PMCA4 at the protein level. When the *Paramecium* sequences are aligned with human PMCA4 (Keeton and Shull, 1995) as a model, it appears that they potentially have the molecular characteristics of a PMCA with 10 transmembrane (TM) spanning regions, acylphosphate intermediate domains, ATP-binding domains, hinge regions and calcium transport regions (see Table S2). There are some exceptions. In ptPMCA4c, a lysine residue for binding ATP is changed to a histidine, and a glutamic acid residue for binding Ca^{2+} in TM4 to an asparagine. In ptPMCA4d, an aspartic acid residue in the acylphosphate intermediate domain is changed to cysteine. In ptPMCA9c, the conserved amino acid 'proline' in the hinge region is changed to a serine.

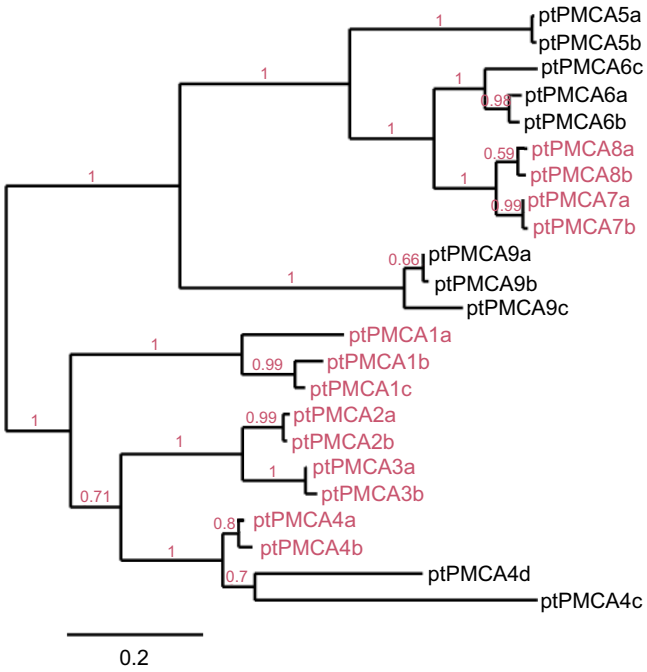

Fig. 1. Phylogeny of plasma membrane Ca^{2+}-ATPases (ptPMCAs) in *Paramecium tetraurelia*. The phylogenic relationships among ptPMCA amino acid sequences were analysed by phylogeny.fr (www.phylogeny.fr). ptPMCAs detected in the ciliary membrane proteomics (Yano et al., 2013) and the present work are shown in red and black, respectively.

The *ptPMCA* family (Fig. 1) falls into two subfamilies (I: paralog groups 1–4; II: paralog groups 5–9). Similarly, there are two subfamilies of *PMCAs* in *Tetrahymena thermophila* (Eisen et al., 2006), suggesting that the two subfamilies separated before differentiation of *Paramecium* and *Tetrahymena*. The members of subfamily II have a short extracellular loop (about 15 amino acids) between TM7 and TM8, similar to mammalian PMCAs. The members of subfamily I have an extended extracellular loop of 50–108 amino acids between TM7 and TM8, which contains 20–35% charged amino acid residues. Such long extracellular loops are found in PMCAs of *T. thermophila* (Eisen et al., 2006) and *Chlamydomonas reinhardtii* (Merchant et al., 2007), and in Ca^{2+}-ATPase of *Plasmodium falciparum* (Krishna et al., 2001).

The C-terminal cytoplasmic tails of all ptPMCAs as well as PMCAs in the other ciliates *T. thermophila* (Eisen et al., 2006) and *P. caudatum* (McGrath et al., 2014) have about 50 amino acids (38–65). These C-terminal tails are much shorter than those in mammalian PMCAs, except for a splice variant of rat, PMCA3f, with 71 amino acids (Burk and Shull, 1992). The ptPMCA C-terminal amino acid sequences vary among paralog groups.

RNAi for 13 ciliary ptPMCAs

While there are 23 genes for *ptPMCAs*, we focused our RNAi study on the sequences of ciliary *ptPMCA1a*, *-1b*, *-1c*, *-2a*, *-2b*, *-3a*, *-3b*, *-4a*, *-4b*, *-7a*, *-7b*, *-8a* and *-8b*, which were found in the ciliary membrane proteome (Yano et al., 2013). We examined indirectly whether any of these ptPMCAs reduce intraciliary Ca^{2+} following the Ca^{2+} action potential by using feeding RNAi and assaying backward swimming behavior in solutions that depolarize and induce action potentials. Once the level of intraciliary Ca^{2+} rises with opening of the ciliary voltage-gated calcium channels during the action potential, the cell will swim backwards due to the changed ciliary power stroke until the intraciliary Ca^{2+} is reduced back to resting levels. Therefore, the duration of backward swimming is a read-out of intraciliary Ca^{2+}.

We designed unique sequences of 200 or more bases for RNAi for each *ptPMCA* gene, except for *ptPMCA3a* and *ptPMCA3b* (Li and Durbin, 2009; Arnaiz and Sperling, 2011). Because there was no unique sequence that would distinguish between these paralogs, we proceeded to silence both together with one sequence (Table S1). While we selected unique sequences for the other genes that should not have off-target effects, we found from examining RT-PCR results (for example Fig. 2B) that secondary siRNAs as predicted by Carradec et al. (2015) must have affected the mRNA levels of paralogs. Therefore, we examined the effects of RNAi for each set of paralogs using RT-PCR (Fig. 2B; Fig. S1) to understand the specificity or lack thereof for the gene silencing.

Cells were fed bacteria transfected with L4440 control (L4440 empty vector that we refer to as *EV*) or L4440 containing a sequence from a *ptPMCA* gene. The summary of the backward swimming assays following this feeding is shown in Table 2. All assays were repeated three times, with the exception of the mixture of all three *ptPMCA1s*, which was performed once.

Journal of Experimental Biology (2021) 224, jeb232074. doi:10.1242/jeb.232074

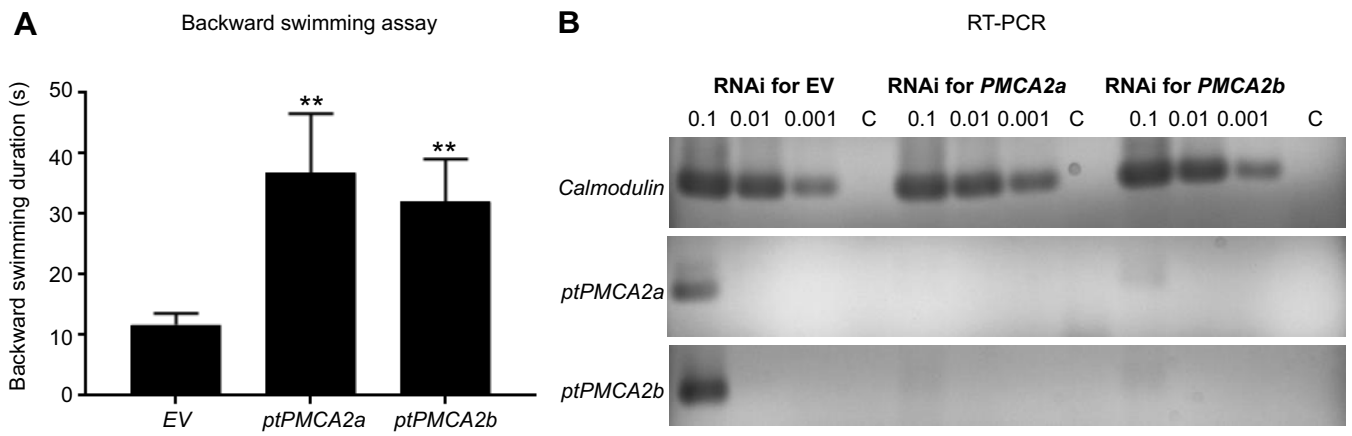

Fig. 2. RNAi treatment of plasma membrane Ca^{2+}-ATPases *ptPMCA2a* and *ptPMCA2b* prolong backward swimming of cells after the action potential. Cells were fed HT115 bacteria transfected with control L4440 (*EV*) or L4440 containing *ptPMCA2* and induced double strand RNA production for 4 h. The backward swimming assay and RT-PCR were carried out at 72 h after feeding. (A) Backward swimming assay; the backward swimming durations (s) are shown as means±s.d. Mann–Whitney *U*-test is used for a statistical test. RNAi for *ptPMCA2a* or *ptPMCA2b* significantly lengthens backward swimming duration (**P<0.001) compared with RNAi for control EV (also see Table 2). (B) RT-PCR: total RNA of 1 µg was used for synthesizing first strand cDNA. First strand cDNA was diluted to 0.1, 0.01 and 0.001 for PCR. 'C' indicates control reaction without reverse transcriptase, diluted to 1:10 for PCR. These results show that RNAi for *ptPMCA2a* or *ptPMCA2b* reduced transcripts of *PMCA2a* and *ptPMCA2b*. *Calmodulin* PCR shows that the input cDNA was same among experiments and was not affected by the RNAi for *ptPMCA2a* or *ptPMCA2b*. This experiment was repeated three times.

The RNAi for either *ptPMCA2a* or *ptPMCA2b* led cells to lengthen the backward swimming duration in 30 mmol l^{-1} KCl by 215 and 175%, respectively (P<0.001) (Fig. 2A). These cells also showed longer backward swimming than the cells fed the *EV* control in other depolarizing solutions (20 mmol l^{-1} NaCl or 20 mmol l^{-1} NaCl/10 mmol l^{-1} TEA-Cl) (Table 3). The RNAi for a mixture of *ptPMCA2a* and *ptPMCA2b* caused a significant increase of backward swimming duration in high-K^+ solutions, but the increase was not additive. The RT-PCR results show that the RNAi for *ptPMCA2a* or *ptPMCA2b* reduced both transcripts, respectively (Fig. 2B), which could explain the loss of additivity when RNAi is used for both genes at once. The calmodulin control RT-PCR shows that the input cDNA was the same among the experiments.

All the rest of the RNAi treatments for the ptPMCAs of the ciliary membrane produced small or no changes in backward swimming. For example, the RNAi-treated cells for *ptPMCA1a* showed slightly longer backward swimming compared with RNAi control cells (P<0.01; Table 2). The RNAi for *ptPMCA1b* and *ptPMCA1c* separately or combined did not show any significant difference in backward swimming duration compared with the RNAi for control *EV*. RNAi for the mixture of *ptPMCA1a* with *ptPMCA1b* or *ptPMCA1b* and *ptPMCA1c* showed slightly longer backward

Table 2. Effects of RNAi for ptPMCA on the duration of backward swimming (s) induced with 30 mmol l^{-1} KCl

RNAi	Mean±s.d. (s)	Cell number	Mann–Whitney *U*-test	Percentage*	RNAi	Mean±s.d. (s)	Cell number	Mann–Whitney *U*-test	Percentage*
EV	12.2±2.3	108			*EV*	11.4±1.9	97		
ptPMCA1a	14.1±3.1	108	*P*<0.01	16	*ptPMCA3a/3b*	12.1±2.9	97	*P*>0.05	
EV	12.8±1.8	105			*EV*	13.0±2.4	129		
ptPMCA1b	12.8±2.3	105	*P*>0.05		*ptPMCA4a*	12.3±2.0	105	*P*>0.05	
ptPMCA1c	12.6±2.0	105	*P*>0.05		*ptPMCA4b*	13.3±2.4	105	*P*>0.05	
EV	11.7±1.7	48			*EV*	12.6±2.6	108		
1a+1b	12.8±1.8	48	*P*<0.05	9	*4a+4b*	13.2±2.6	108	*P*>0.05	
EV	10.9±1.3	48			*EV*	11.6±1.5	109		
1a+1c	11.4±1.9	48	*P*>0.05		*ptPMCA7a*	11.8±2.0	109	*P*>0.05	
					ptPMCA7b	11.8±2.2	109	*P*>0.05	
EV	11.2±2.1	65							
1b +1c	10.0±1.9	65	*P*>0.05		*EV*	11.1±2.1	193		
					7a+7b	11.2±1.8	193	*P*>0.05	
Ev	10.4±1.1	12							
1a+1b+1c	12.0±1.6	12	*P*<0.05	15	*EV*	12.2±2.1	158		
					ptPMCA8a	11.6±1.8	158	*P*<0.05	–5
EV	11.7±1.9	130			*ptPMCA8b*	11.7±1.8	158	*P*>0.05	
ptPMCA2a	36.8±9.8	96	*P*<0.001	214					
ptPMCA2b	32.0±7.1	97	*P*<0.001	174	*EV*	12.9±2.4	96		
					8a+8b	12.3±1.9	96	*P*>0.05	
EV	12.4±2.4	37							
2a+2b	32.0±4.1	37	*P*<0.001	158					
1a+2a+2b	32.4±3.6	25	*P*<0.001	161					

*When there was a statistical difference between control (*EV*, empty vector) RNAi and test (*PMCA*) RNAi, the difference is shown as (mean test duration–mean control duration)/control duration×100%. The experiment of EV versus 1a+1b+c was performed once. All others were repeated at least three times.

Journal of Experimental Biology (2021) 224, jeb232074. doi:10.1242/jeb.232074

Table 3. Effects of RNAi for *ptPMCA2a* and *ptPMCA2b* on backward swimming behavior in various depolarizing conditions

Solution	RNAi for EV	RNAi for *ptPMCA2a* and *ptPMCA2b*
1 mmol l^{-1} Ba^{2+}	Barium dance (*N*=30)	Single long backward (*N*=30)*
30 mmol l^{-1} Na^{+}	Jerky (*N*=30)	11.4±6.7 s (*N*=27)
20 mmol l^{-1} Na^{+} and 10 mmol l^{-1} TEA	17.4±13.8 s (*N*=75)	33.9±26.3 s (*N*=74)

P<0.001, Mann–Whitney *U*-test. *RNAi cells for *ptPMCA2a* and *ptPMCA2b* swim longer backwards for 3–5 s in each episode of barium dances compared with less than 1 s in each one in the control RNAi cells. The experiments were repeated three times.

swimming duration ($P<0.05$). This effect may be due to the silencing of *ptPMCA1a* alone. The results of RT-PCR show the RNAi for each *ptPMCA1* gene causes the reduction of its transcript, but does not affect the others (Fig. S1A1–3).

The RNAi for the individual paralogs *ptPMCA3*, *ptPMCA4* or *ptPMCA7* and the mixture of paralog members did not show significantly longer backward swimming duration compared with the RNAi for *EV* ($P>0.05$; Table 2). The RNAi for *ptPMCA8a* even showed slightly shorter backward swimming ($P<0.05$; Table 2), but a mixture of *ptPMCA8a* and *ptPMCA8b* did not show a difference compared with cells treated with RNAi for *EV* ($P>0.05$).

From RT-PCR, the RNAi for individual genes for paralog groups *ptPMCA3*, *ptPMCA4*, *ptPMCA7* or *ptPMCA8* down-regulated its transcripts and those of its paralog partner (Fig. S1B,D1–2,E,F). The RNAi for ptPMCA4a reduced its transcript, but did not affect the transcript of ptPMCA4b, and vice versa (Fig. S1C).

PMCA2a and *PMCA2b* co-IP with channels Ca_V1b and Ca_V1c

The *Paramecium* Ca_V channels are in low abundance in the cilia, making their peptides difficult to detect by LC-MS/MS analysis (Yano et al., 2013). However, low abundance transmembrane proteins can be extracted by the detergent Triton X-114 (Yano et al., 2013). We found that using Triton X-114 coupled with over-expression of tagged channels made it possible for us to detect ciliary Ca_V channels and test for potential interactions with other ciliary proteins by IPs from cells over-expressing the tagged Ca_V1a, Ca_V1b and Ca_V1c (Lodh et al., 2016; Valentine et al., 2012; Yano et al., 2013). Note that *Ca_V1a* and *Ca_V1b* are ohnologs with 87% identity at the nucleotide level. We cannot distinguish them for RNAi or their proteins using LC-MS/MS. *Ca_V1c* is 75% identical to *Ca_V1a* and *Ca_V1b* and can be distinguished from *Ca_V1a* and *Ca_V1b* (Lodh et al., 2016). Therefore, we focus on Ca_V1b and Ca_V1c, and have not repeated these experiments with Ca_V1a.

With this combined approach of over-expression and Triton X-114 extraction, we created two ciliary supernatants from cells expressing FLAG-Ca_V1b or FLAG-Ca_V1c. From these we precipitated proteins with anti-FLAG M2 gel for the FLAG-channels or anti-ptPMCA2a (2aN pAb). Cells expressing only FLAG provided the control ciliary supernatants. Detection on blots utilized FLAG monoclonal antibody (mAb), FLAG pAb or 2aN pAb. Fig. 3 shows the results. These experiments were repeated three times.

In Fig. 3A, the IPs with FLAG M2 gel were performed using cilia from cells expressing FLAG-Ca_V1b, or FLAG-Ca_V1c, or FLAG. Fig. 3Ai and Aiii show that the channel FLAG-Ca_V1b or FLAG-CaV1c (arrow at ∼270 kDa corresponding to the expected mass for the channels) is only detected by FLAG pAb from cells expressing FLAG-Ca_V1b or FLAG-Ca_V1c, respectively, and not expressing FLAG alone. When the blots from these IPs are probed with 2aN pAb, there are bands of the appropriate mass (∼132 kDa) for pumps *ptPMCA2a/b* in the lane from cells expressing FLAG-Ca_V1b or FLAG-Ca_V1c, but not from those expressing FLAG (Fig. 3Aii and Aiv). Hence, the pumps ptPMCA2a and ptPMCA2b appear to co-IP with the channels Ca_V1b and Ca_V1c.

In Fig. 3B, a reciprocal set of experiments was performed using 2aN pAb to IP from the supernatants from cilia of cells expressing FLAG-Ca_V1b, or FLAG-Ca_V1c or FLAG. The blots from IPs with 2aN pAb were probed with 2aN pAb and FLAG mAb. Fig. 3Bi and Biii show the band of about 132 kDa corresponding to the mass of ptPMCA2a/2b are detected with 2aN pAb in both lanes from cells expressing FLAG-Ca_V1b, or FLAG-Ca_V1c, and FLAG. This latter results because all these supernatants including from cells expressing only FLAG have endogenous ptPMCAs. Fig. 3Bii and Biv show that when the blots from these IPs were probed with FLAG mAb, there is a band of about 270 kDa corresponding to the mass of FLAG-Ca_V1b or FLAG-Ca_V1c only in the IPs from cells expressing FLAG-Ca_V1b or FLAG-Ca_V1c but not from cells expressing FLAG, respectively.

While the bands detected on western blots by the FLAG or 2aN antibodies should be evidence of the presence of the Ca_V1 subunits or the ptPMCA2a or ptPMCA2b in Fig. 3, we also ran silver-stained gels in parallel with the western blots and analysed the regions with the bands by LC-MS/MS. We did this for the proteins from IPs in Fig. 3A, iii and iv. Multiple peptides for Ca_V1c were detected in the region of the ∼270 kDa bands from the IP with FLAG M2 gel from cilia expressing FLAG-Ca_V1c in Fig. 3Aiii (Table S3A). The weak band lower than 270 kDa in Fig. 3Aiii detected in only the test lane might be a degraded product from FLAG-Ca_V1c. We have confidence that the channel proteins are in the 270 kDa region.

Likewise, peptides for ptPMCA2a and/or ptPMCA2b were identified by LC-MS/MS from the region around 130 kDa in Fig. 3Aiv (Table S3B). All the peptides identified match with ptPMCA2a or ptPMCA2b. A minority are not unique to ptPMCA2 and can also be found in ptPMCA3 or ptPMCA4, but none is unique to ptPMCA3 or ptPMCA4. The lowest two bands of 120 kDa in Fig. 3Aiv appear to be non-specific because they are in both the control and test lanes. Thus, the Ca_V channel Ca_V1c appears to co-IP with ptPMCA2a/2b.

In Fig. 3C, the loading controls for the co-IP experiments of FLAG-Ca_V1b versus FLAG and FLAG-Ca_V1c versus FLAG, are shown for the α-tubulin in Triton X-114 extracts before that IP was performed. It appears that less material was loaded in the cells expressing FLAG-Ca_V1c (Fig. 3Cii), not changing the general outcome, but making the band in Fig. 3B, iii and iv an underestimate.

OptiPrep density gradient

DRMs from the cilia expressing FLAG-Ca_V1c were subjected to OptiPrep density step gradients and analysed by western blotting. The sAG_51B antibody was used to identify a GPI-anchored surface antigen sAG_51B (Capdeville and Benwakrim, 1996). Although GPI anchored proteins can be associated with lipid rafts or liquid-ordered DRM domains in other organisms, here we use this protein as a marker of the membrane as opposed to intraciliary or intracellular proteins (Brown and London, 1998; Hooper, 1999; Zurzolo and Simons, 2016). This protein (250 kDa) was distributed in fractions 1, 2, 4, 5 and 6 (Fig. 4A). Both FLAG-Ca_V1c (∼270 kDa) and ptPMCA2a and ptPMCA2b (∼132 kDa) were located in fractions 4 and 5 (Fig. 4B,C). In Fig. 4C, additional bands, 128 and 150 kDa, were detected.

Journal of Experimental Biology (2021) 224, jeb232074. doi:10.1242/jeb.232074

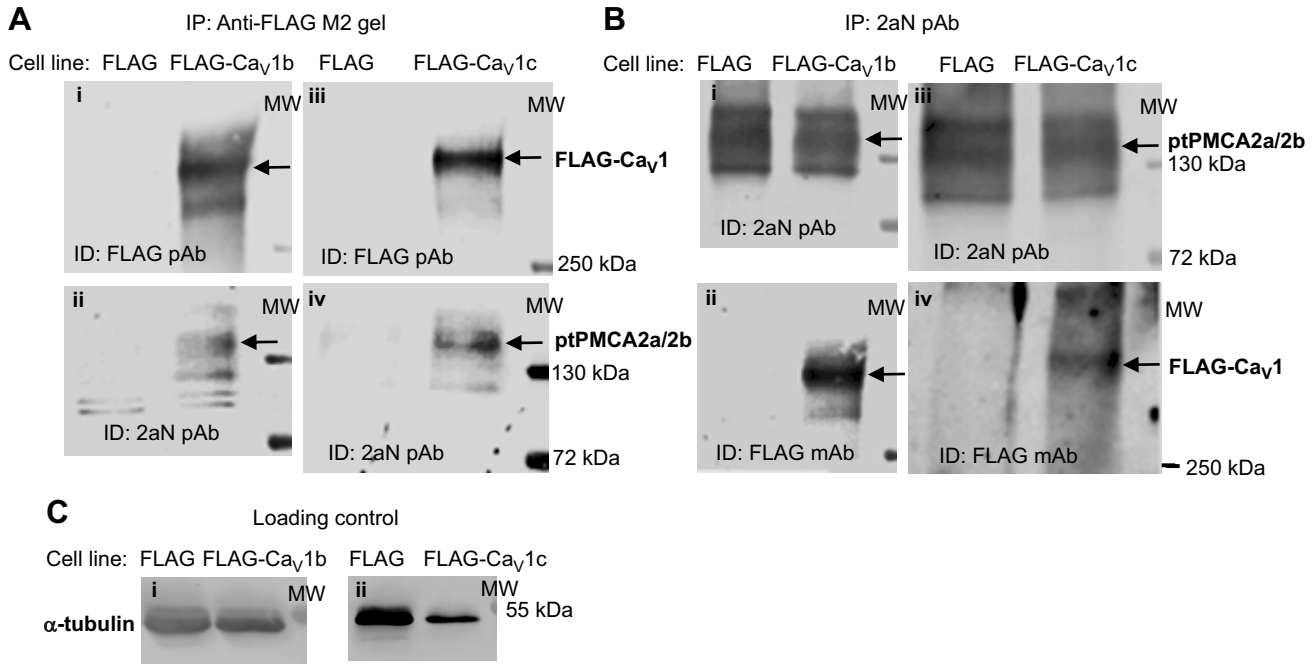

Fig. 3. Plasma membrane Ca^{2+}-ATPase (ptPMCA2a and ptPMCA2b) co-IP with voltage-gated Ca^{2+} channel α1 subunits (Ca_V1b and Ca_V1c). We examined the potential for interaction of these PMCAs and ciliary Ca_V channels using the IP from a Triton X-114 solubilization of ciliary membranes using FLAG M2 and 2aN pAb and western blot analysis. Molecular mass markers were run in parallel, and are shown in the right-most lane of each panel. ID, immunodetection; mAb, monoclonal antibody; pAb, polyclonal antibody; MW, molecular weight marker. This experiment was repeated three times. (A) For the IPs with FLAG M2 gels and western blots were performed using cilia from cells expressing FLAG-Ca_V1b, or FLAG-Ca_V1c, or FLAG. (Ai,Aiii) The channel FLAG-Ca_V1b or FLAG-Ca_V1c (arrow at about 270 kDa corresponding to the expected mass for FLAG-Ca_V1b) is only detected by FLAG pAb in the IPs of cilia supernatants from cells expressing FLAG-Ca_V1b or FLAG-Ca_V1c, respectively. When the blots from these IPs are probed with 2aN pAb, there is a band of the appropriate mass (about 132 kDa) for pumps ptPMCA2a and ptPMCA2b in the lane from cells expressing FLAG-Ca_V1b but not from those expressing FLAG (Aii,Aiv). Hence, the pumps ptPMCA2a and ptPMCA2b appear to co-IP with the channels Ca_V1b and Ca_V1c. (B) The blots from IPs with 2aN pAb were probed with 2aN pAb and FLAG mAb. (Bi,Biii) The band of about 132 kDa corresponding to the mass of ptPMCA2a and ptPMCA2b is detected with 2aN pAb in both lanes from cells expressing FLAG-Ca_V1b, or FLAG-Ca_V1c, and FLAG. (The antibody 2aN is against a pump peptide, which means that the endogenous pumps will be precipitated from the supernatants of FLAG channel and FLAG-expressing cells.) (Bii,Biv) When the blots from these IPs were probed with FLAG mAb, there is a band of about 270 kDa corresponding to the mass of FLAG-Ca_V1a or FLAG-Ca_V1c only in the IPs from cells expressing FLAG-Ca_V1a or FLAG-Ca_V1c but not from cells expressing FLAG, respectively. Hence, the FLAG channels appear to co-IP with the pumps. (C) The loading controls are shown for α-tubulin of the Triton X-114 extracts before the IPs for FLAG-Ca_V1b versus FLAG and FLAG-Ca_V1c versus FLAG were performed. (Ci,Cii) Relative amounts of α-tubulin solubilized with Triton X-114.

Alpha-tubulin (50 kDa) was identified in fractions 4, 5, 6 and 8 (Fig. 4D). The experiments were performed in triplicate.

DISCUSSION

PMCAs in *Paramecium* cilia and their role in removing Ca^{2+} following the Ca^{2+} action potential

It has been suggested that the Ca^{2+} entering *Paramecium* cilia through Ca_V channels during the action potential is actively removed by calcium pumps (Doughty and Dryl, 1981; Eckert and Brehm, 1979). Other means of reducing Ca^{2+} after the action potential have also been suggested, such as binding to calmodulin or centrin (Plattner, 2015). However, our interest was to examine the possible roles of PMCAs in this important regulation of Ca^{2+} in ciliary beating.

Paramecium tetraurelia has many (23) genes encoding plasma membrane Ca^{2+}-ATPase (ptPMCA) (Table 1), which have the same molecular characteristics as mammalian PMCAs, such as acylphosphate intermediate and calcium transport domains (Table S2). Past proteomic studies of cilia identified 13 ptPMCAs in cilia and also show that ptPMCA2a and ptPMCA2b are enriched in cilia (Arnaiz and Sperling, 2011; Lodh, 2012; Yano et al., 2013, 2015). Among these ptPMCAs, only the transcripts of *ptPMCA2a* and *ptPMCA2b* are significantly induced during reciliation (Arnaiz et al., 2010). While these results point to ptPMCA2a and ptPMCA2b for roles in regulating Ca^{2+} in *Paramecium* cilia, we applied RNAi studies to all 13 ciliary ptPMCAs.

We used high K^+ solutions to initiate depolarizations strong enough to open the Ca_V channels, which are exclusively in the cilia, and trigger an action potential (Dunlap, 1977). The Ca^{2+} entering through these channels affects the axonemes and the power stroke of the cilia, causing the cell to swim backwards. Action potentials are graded, meaning that the Ca^{2+} in the cilia and the duration of this backward swimming is proportional to the activity of Ca_V channels (Haga et al., 1984; Satow and Kung, 1980). The resting membrane potential is quickly restored after the action potential by voltage-gated and calcium activated potassium channels (Brehm et al., 1978; Oertel et al., 1977; Satow and Kung, 1980). However, backward swimming continues until intraciliary calcium is returned to 100 nmol l^{-1} or less (Eckert, 1972). This relationship allows us to use the duration of backward swimming as a bioassay for Ca^{2+} lingering in the cilia after the action potential.

Our results with RNAi support the hypothesis that ptPMCAs are involved in regulating intraciliary Ca^{2+} from the calcium action potential. We found that RNAi depletion of *ptPMCA2a* and *ptPMCA2b* causes cells in depolarizing conditions (e.g. high K^+) to

Journal of Experimental Biology (2021) 224, jeb232074. doi:10.1242/jeb.232074

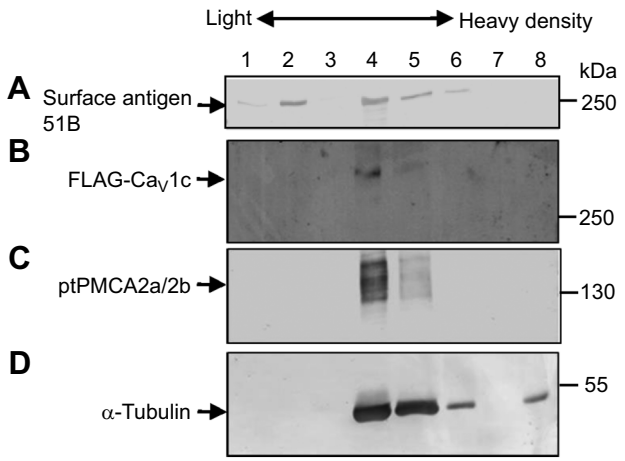

Fig. 4. PMCA2a/2b and Ca_V1c found in same fractions of OptiPrep density gradient. Cilia isolated from cells expressing FLAG-Ca_V1c were treated with 1% Triton X-100 at 4°C for 1 h. The detergent-resistant ciliary membranes were floated in iodixanol (OptiPrep) discontinuous density gradients (see Materials and Methods for detail). Eight fractions were analysed on western blots using surface antigen 51B (sAG_51B) pAb, 2aN pAb, FLAG pAb and α-tubulin mAb. sAG_51B is a glycosylphosphatidylinositol (GPI)-anchored protein, which was used as a peripheral membrane protein marker. sAG_51B (250 kDa) was distributed in fractions 2, 4, 5 and 6 (A), α-tubulin (50 kDa) in fractions 4, 5, 6 and 8 (D), and ptPMCA2a and ptPMCA2b (132 kDa) and Ca_V1c (270 kDa) in fractions 4 and 5, respectively (B and C). This experiment was repeated times.

prolong backward swimming compared with cells treated with RNAi for *EV* (Fig. 2; Table 2). RNAi for the other 11 *ptPMCAs* had little or no impact on the duration of backward swimming. Despite sharing conserved domains with ptPMCA2a and ptPMCA2b (Table 1), the other 11 ciliary ptPMCAs apparently cannot compensate when these two ptPMCAs are reduced. RNAi for *ptPMCA2a* and *ptPMCA2b* also results in significantly longer backward swimming induced by other depolarizing stimuli such high Na^+ and Na^+/TEA (Table 3). Likewise, with the depolarizing stimulus Ba^{2+}, RNAi for *ptPMCA2a* and *ptPMCA2b* resulted in longer backward swimming in the barium dance, which is a bout of repeated backward swimming (Kung et al., 1975). Thus, ptPMCA2a and ptPMCA2b appear to participate in regulating Ca^{2+} concentration in the cilia for the ciliary beat or reversal.

ptPMCA2a and ptPMCA2b may be co-located in the ciliary membrane with two voltage-gated calcium channel α1 subunits

Paramecium voltage-gated Ca_V channels of the action potential are limited to the cilia (Dunlap, 1977). We identified three Ca_V channel α1 subunits from the cilia (Yano et al., 2013) and expressed them as epitope-tagged proteins in the cilia (Lodh et al., 2016). Two of these subunits were almost identical in sequence, which allowed us to follow all three by focusing on just two: Ca_V1b and Ca_V1c.

The ptPMCA2a and ptPMCA2b co-IP with Ca_V channel α1 subunits Ca_V1b and Ca_V1c and vice versa (Fig. 3). We refer to these as reciprocal IPs. When we used LC-MS/MS to analyse the proteins that were precipitated with the antibodies against the FLAG channels or pumps, we found that some peptides could also be from ptPMCA3s and ptPMCA4s (Table S3). However, these were not unique to these pumps and were in common with ptPMCA2a and ptPMCA2b. RNAi for ptPMCA3s and ptPMCA4s did not affect the backward swimming behavior (Fig. 2). Therefore, we focused on ptPMCA2a and ptPMCA2b below. We suggest that there is a proximity of these two pumps and the Ca_V channels sufficient for co-IP. We cannot comment on whether there is a physical interaction or novel protein connecting ptPMCA2a/ptPMCA2b and the Ca_V channels that allow them to co-IP.

The proximity of ptPMCA2s and the Ca_V channels in *Paramecium* ciliary membranes could affect the activity of the Ca_V channels because the Ca_V channels are known to be inactivated by the Ca^{2+} from the action potential (Brehm and Eckert, 1978). Thus, if the ptPMCAs were physically close to the Ca_V channels they could quickly remove Ca^{2+} from the vicinity of the channel and prepare the channel for the next excitatory action potential. The potential interactions of the channels with ptPMCAs possibly would not require Ca^{2+} because the reciprocal IPs were done in the absence of Ca^{2+} (free Ca^{2+}<10^{-10} mol l^{-1} in the membrane buffer and FLAP200) implying that ptPMCA2a and ptPMCA2b are in proximity with Ca_V channels while the pumps are in a resting state.

The ptPMCAs and Ca_V channels are large transmembrane proteins, and it is logical that they both partition into the Triton-X114 detergent fraction that we use to concentrate transmembrane proteins for IPs (Yano et al., 2013). However, we do not believe that this process of concentration is solely responsible for their proximity, allowing them to co-IP. A different approach using OptiPrep density fractions likewise implied that ptPMCA2a and ptPMCA2b, and Ca_V channel α1 subunits Ca_V1b and Ca_V1c are in the same 'neighborhoods' of the ciliary membrane.

The lipid microdomains called rafts are small (10–200 nm), heterogeneous, highly dynamic, sterol- and sphingolipid/cholesterol-enriched domains that compartmentalize cellular processes (Pike, 2006; Sezgin et al., 2017; Simons and Toomre, 2000). The lipid rafts serve to concentrate proteins together to facilitate reactions (Simons and Toomre, 2000) and organize various calcium signaling pathways (see Pani and Singh, 2009). PMCAs in general have been found to localize in lipid rafts. For example, mammalian PMCA4 is found in light-density lipid rafts in Nycodenz gradients of pig cerebellum synaptic membranes, and has a higher activity than when in the heavier fraction (Sepúlveda et al., 2006). All four isoforms of rat primary cortical neuron PMCAs localize in lipid rafts (i.e. in light density fraction in sucrose density gradient), and activity is much higher for the PMCAs in rafts than for those outside rafts domains (e.g. heavy density membrane fractions) (Jiang et al., 2007).

Paramecium cilia and potential lipid domains

Ciliary membranes, such as those from *Trypanosoma* flagella (Tyler et al., 2009) and the primary cilia of epithelial cells, have lipid domains (Janich and Corbeil, 2007). The lipid composition of the *Paramecium* ciliary membrane is also specifically conducive to lipid raft formation (Kaneshiro, 1987).

We analysed the fraction of *Paramecium* ciliary membranes that is resistant to cold Triton X-100, i.e. DRMs (Simons and Toomre, 2000), and further separated them by density using OptiPrep density gradients. We noted the distribution of sAG_51B, which is a glycosylphosphatidylinositol (GPI)-anchored protein (Capdeville and Benwakrim, 1996). These peripheral membrane proteins in other systems are hallmarks of lipid rafts (Brown and London, 1998; Hooper, 1999; Simons and Toomre, 2000; Zurzolo and Simons, 2016). However, in our studies, the sAG_51B is found not only in light fractions characteristic of rafts but also in two heavier density fractions (Fig. 4). The ptPMCA2a and ptPMCA2b as well as Ca_V channels are found with the sAG_51B antigen in intermediate density fraction 4 (Fig. 4). We do not know the significance of this localization or that of tubulin in the same density fraction as

ptPMCAs. However, tubulin may play a negative role in PMCA activity control as PMCAs are inhibited by acetylated tubulin in the plasma membrane vesicles isolated from brain synapses (Monesterolo et al., 2008). In previous studies using Triton X-114 to solubilize integral ciliary membrane proteins for proteomic analysis, we found tubulin together with the transmembrane proteins such as ptPMCA2a, ptPMCA2b and Ca_V1c partitioned into the detergent phase (Yano et al., 2013).

A *Paramecium* membrane protein, stomatin, is associated with lipid rafts (Reuter et al., 2013). The behavioral effects of the depletion of stomatin 1 show a clear role for this protein in *Paramecium* cell body (versus cilia) membrane function. The loss of stomatin 1 leads to reduction in the anterior mechanosensory response, which is initiated by a depolarizing receptor potential. However, stomatin 1 is absent from the cilia and its RNAi phenotype can be explained by reduction of the receptor potential and not by a direct effect on cilia or their channels.

Calcium-binding proteins

Ciliary reversal requires intraciliary free Ca^{2+} to rise to between 10 µmol l^{-1} and 1 mmol l^{-1} from a resting level of 100 nmol l^{-1} (Eckert, 1972; Kung and Naitoh, 1973; Naitoh and Kaneko, 1972). This ciliary Ca^{2+} must then be returned to the resting level of 100 nmol l^{-1} or less (Eckert, 1972). As the Ca^{2+} does not spill out into the cytoplasm (Husser et al., 2004), it has been suggested that the Ca^{2+} entering during the action potential is actively removed by calcium pumps or sequestered by calcium-binding proteins such as calmodulin or centrin (Doughty and Dryl, 1981; Eckert and Brehm, 1979; Plattner, 2015).

Although we believe that our study shows that at least two ptPMCAs are involved in the process of returning ciliary Ca^{2+} to rest, our study does not address or eliminate calcium-binding proteins (Plattner, 2015) from playing roles in ciliary Ca^{2+} regulation.

Conclusions

Of 23 ptPMCAs, ptPMCA2a and ptPMCA2b are most abundant in the cilia. They are located in the ciliary membrane close enough or with sufficient interactions to the Ca_V channels for co-IP. In addition, the pumps and channels are found in the same membrane density fractions. RNAi depletion implicates ptPMCA2a and ptPMCA2b in the reduction of intraciliary Ca^{2+} after the calcium action potential. We propose that the pumps are critically positioned to quickly remove Ca^{2+} and ready the cilium for the next action potential. The channels are inhibited by Ca^{2+} and removal of this Ca^{2+} is essential for the next round of excitation (Brehm et al., 1978; Klumpp et al., 1990). Although a demonstration of co-localization of the ptPMCAs and Ca_V channels in membrane fractions such as lipid rafts requires additional studies, we believe that our study shows that at least two ptPMCAs are involved in the process of returning ciliary Ca^{2+} to rest. Our study does not discount calcium-binding proteins (Plattner, 2015) from playing roles in ciliary Ca^{2+} regulation.

Acknowledgements

We thank Ms C. Hood for helping with LC-MS/MS.

Competing interests

The authors declare no competing or financial interests.

Author contributions

Conceptualization: J.Y., J.L.V.H.; Methodology: J.Y., Y.-W.L., J.L.V.H.; Software: Y.-W.L.; Validation: J.Y., R.W., Y.-W.L., J.L.V.H.; Formal analysis: J.Y., Y.-W.L., J.L.V.H.; Investigation: J.Y., R.W., Y.-W.L., J.L.V.H.; Resources: J.Y., R.W., Y.-W.L., J.L.V.H.; Data curation: J.Y., R.W., Y.-W.L., J.L.V.H.; Writing - original draft: J.Y., J.L.V.H.; Writing - review & editing: J.Y., R.W., Y.-W.L., J.L.V.H.; Visualization: J.Y., Y.-W.L., J.L.V.H.; Supervision: J.L.V.H.; Project administration: J.L.V.H.; Funding acquisition: J.L.V.H.

Funding

Research reported in this publication was supported by an Institutional Development Award (IDeA) from the National Institute of General Medical Sciences (NIGMS) of the National Institutes of Health (NIH) under grant number P20GM103449 to J.L.V.H. for mass analysis, and NCI P30CA22435 for DNA sequencing. Deposited in PMC for release after 12 months.

References

Arnaiz, O. and Sperling, L. (2011). ParameciumDB in 2011: new tools and new data for functional and comparative genomics of the model ciliate *Paramecium tetraurelia*. *Nucleic Acids Res.* **39**, D632-D636. doi:10.1093/nar/gkq918

Arnaiz, O., Goût, J.-F., Bétermier, M., Bouhouche, K., Cohen, J., Duret, L., Kapusta, A., Meyer, E. and Sperling, L. (2010). Gene expression in a paleopolyploid: a transcriptome resource for the ciliate *Paramecium tetraurelia*. *BMC Genomics* **11**, 547-547. doi:10.1186/1471-2164-11-547

Arnaiz, O., Meyer, E. and Sperling, L. (2020). ParameciumDB 2019: integrating genomic data across the genus for functional and evolutionary biology. *Nucleic Acids Res.* **48**, D599-D605. doi:10.1093/nar/gkz948

Aury, J., Jaillon, O., Duret, L., Noel, B., Jubin, C., Porcel, B., Segurens, B., Daubin, V., Anthouard, V., Aiach, N. et al. (2006). Global trends of whole-genome duplications revealed by the ciliate *Paramecium tetraurelia*. *Nature* **444**, 171-178. doi:10.1038/nature05230

Blaustein, M. P. and Lederer, W. J. (1999). Sodium/calcium exchange: its physiological implications. *Physiol. Rev.* **79**, 763-854. doi:10.1152/physrev.1999.79.3.763

Brehm, P. and Eckert, R. (1978). Calcium entry leads to inactivation of calcium channel in *Paramecium*. *Science* **202**, 1203-1206. doi:10.1126/science.103199

Brehm, P., Dunlap, K. and Eckert, R. (1978). Calcium-dependent repolarization in *Paramecium*. *J. Physiol.* **274**, 639-654. doi:10.1113/jphysiol.1978.sp012171

Brini, M. and Carafoli, E. (2011). The plasma membrane Ca^{2+} ATPase and the plasma membrane sodium calcium exchanger cooperate in the regulation of cell calcium. *Cold Spring Harb. Perspect. Biol.* **3**, a004168. doi:10.1101/cshperspect.a004168

Brown, D. A. (2006). Lipid rafts, detergent-resistant membranes, and raft targeting signals. *Physiology* **21**, 430-439. doi:10.1152/physiol.00032.2006

Brown, D. A. and London, E. (1998). Functions of lipid rafts in biological membranes. *Annu. Rev. Cell Dev. Biol.* **14**, 111-136. doi:10.1146/annurev.cellbio.14.1.111

Burk, S. E. and Shull, G. E. (1992). Structure of the rat plasma membrane Ca^{2+}-ATPase isoform 3 gene and characterization of alternative splicing and transcription products. Skeletal muscle-specific splicing results in a plasma membrane Ca^{2+}-ATPase with a novel calmodulin-binding domain. *J. Biol. Chem.* **267**, 19683-19690. doi:10.1016/S0021-9258(18)41829-7

Calì, T., Brini, M. and Carafoli, E. (2017). Regulation of cell calcium and role of plasma membrane calcium ATPases. *Int. Rev. Cell Mol. Biol.* **332**, 259-296. doi:10.1016/bs.ircmb.2017.01.002

Capdeville, Y. and Benwakrim, A. (1996). The major ciliary membrane proteins in *Paramecium primaurelia* are all glycosylphosphatidylinositol-anchored proteins. *Eur. J. Cell Biol.* **70**, 339-346.

Carradec, Q., Götz, U., Arnaiz, O., Pouch, J., Simon, M., Meyer, E. and Marker, S. (2015). Primary and secondary siRNA synthesis triggered by RNAs from food bacteria in the ciliate *Paramecium tetraurelia*. *Nucleic Acids Res.* **43**, 1818-1833. doi:10.1093/nar/gku1331

Carafoli, E. (1994). Biogenesis: plasma membrane calcium ATPase: 15 years of work on the purified enzyme. *FASEB, J.* **8**, 993-1002. doi:10.1096/fasebj.8.13.7926378

Di Leva, F., Domi, T., Fedrizzi, L., Lim, D. and Carafoli, E. (2008). The plasma membrane Ca^{2+} ATPase of animal cells: structure, function and regulation. *Arch. Biochem. Biophys.* **476**, 65-74. doi:10.1016/j.abb.2008.02.026

Doughty, M. J. and Dryl, S. (1981). Control of ciliary activity in *Paramecium*: an analysis of chemosensory transduction in a eukaryotic unicellular organism. *Prog. Neurobiol.* **16**, 1-115. doi:10.1016/0301-0082(81)90008-3

Dunlap, K. (1977). Localization of calcium channels in *Paramecium caudatum*. *J. Physiol.* **271**, 119-133. doi:10.1113/jphysiol.1977.sp011993

Eckert, R. (1972). Bioelectric control of ciliary activity. *Science* **176**, 473-481. doi:10.1126/science.176.4034.473

Eckert, R. and Brehm, P. (1979). Ionic mechanisms of excitation in *Paramecium*. *Ann. Rev. Biophys. Bioeng.* **8**, 353-383. doi:10.1146/annurev.bb.08.060179.002033

Eisen, J. A., Coyne, R. S., Wu, M., Wu, D., Thiagarajan, M., Wortman, J. R., Badger, J. H., Ren, Q., Amedeo, P., Jones, K. M. et al. (2006). Macronuclear genome sequence of the ciliate *Tetrahymena thermophila*, a model eukaryote. *PLoS Biol.* **4**, e286. doi:10.1371/journal.pbio.0040286

Elwess, N. L. and Van Houten, J. L. (1997). Cloning and molecular analysis of the plasma membrane Ca^{2+}-ATPase gene in *Paramecium tetraurelia*. *J. Eukaryot. Microbiol.* **44**, 250-257. doi:10.1111/j.1550-7408.1997.tb05708.x
Haga, N., Forte, M., Saimi, Y. and Kung, C. (1984). Characterization of cytoplasmic factors which complement Ca^{2+} channel mutations in *Paramecium tetraurelia*. *J. Neurogenet.* **1**, 259-274. doi:10.3109/01677068409107091
Hooper, N. M. (1999). Detergent-insoluble glycosphingolipid/cholesterol-rich membrane domains, lipid rafts and caveolae (Review). *Mol. Membr. Biol.* **16**, 145-156. doi:10.1080/096876899294607
Janich, P. and Corbeil, D. (2007). GM1 and GM3 gangliosides highlight distinct lipid microdomains within the apical domain of epithelial cells. *FEBS Lett.* **581**, 1783-1787. doi:10.1016/j.febslet.2007.03.065
Jiang, L., Fernandes, D., Mehta, N., Bean, J. L., Michaelis, M. L. and Zaidi, A. (2007). Partitioning of the plasma membrane Ca^{2+}-ATPase into lipid rafts in primary neurons: effects of cholesterol depletion. *J. Neurochem.* **102**, 378-388. doi:10.1111/j.1471-4159.2007.04480.x
Husser, M. R., Hardt, M., Blanchard, M.-P., Hentschel, J., Klauke, N. and Plattner, H. (2004). One-way calcium spill-over during signal transduction in *Paramecium* cells: from the cell cortex into cilia, but not in the reverse direction. *Cell Calcium* **36**, 349-358. doi:10.1016/j.ceca.2004.02.003
Kaneshiro, E. S. (1987). Lipids of *Paramecium*. *J. Lipid Res.* **28**, 1241-1258. doi:10.1016/S0022-2275(20)38590-4
Keeton, T. P. and Shull, G. E. (1995). Primary structure of rat plasma membrane Ca^{2+}-ATPase isoform 4 and analysis of alternative splicing patterns at splice site A. *Biochem. J.* **306**, 779-785. doi:10.1042/bj3060779
Kenworthy, A. K. (2020). Choosing who can ride the raft. *Nature Rev. Mol. Cell Biol.* **21**, 566-567. doi:10.1038/s41580-020-00285-y
Klumpp, S., Cohen, P. and Schultz, J. E. (1990). Okadaic acid, an inhibitor of protein phosphatase in *Paramecium*, causes sustained Ca^{2+}-dependent backward swimming in response to depolarizing stimuli. *EMBO J.* **9**, 685-689. doi:10.1002/j.1460-2075.1990.tb08160.x
Krishna, S., Woodrow, C., Webb, R., Penny, J., Takeyasu, K., Kimura, M. and East, J. M. (2001). Expression and functional characterization of a *Plasmodium falciparum* Ca^{2+}-ATPase (PfATP4) belonging to a subclass unique to apicomplexan organisms. *J. Biol. Chem.* **276**, 10782-10787. doi:10.1074/jbc.M010554200
Kung, C. and Naitoh, Y. (1973). Calcium-induced ciliary reversal in the extracted models of 'Pawn', a behavioral mutant of *Paramecium*. *Science* **179**, 195-196. doi:10.1126/science.179.4069.195
Kung, C., Chang, S., Satow, Y., Houten, J. and Hansma, H. (1975). Genetic dissection of behavior in *Paramecium*. *Science* **188**, 898-904.
Levental, I., Levental, K. R. and Heberle, F. A. (2020). Lipid rafts: controversies resolved, mysteries remain. *Trends Cell Biol.* **30**, 341-353. doi:10.1016/j.tcb.2020.01.009
Li, H. and Durbin, R. (2009). Fast and accurate short read alignment with Burrows–Wheeler transform. *Bioinformatics* **25**, 1754-1760. doi:10.1093/bioinformatics/btp324
Lodh, S. (2012). Characterization of PWA and PWB proteins in *Paramecium*. *PhD thesis, University of Vermont*, Burlington, VT, USA.
Lodh, S., Yano, J., Valentine, M. S. and Van Houten, J. L. (2016). Voltage-gated calcium channels of *Paramecium* cilia. *J. Exp. Biol.* **219**, 3028-3038. doi:10.1242/jeb.141234
Lopreiato, R., Giacomello, M. and Carafoli, E. (2014). The plasma membrane calcium pump: new ways to look at an old enzyme. *J. Biol. Chem.* **289**, 10261-10268. doi:10.1074/jbc.O114.555565
Machemer, H. (1988). Electrophysiology. In *Paramecium* (ed. H.-D. Gortz), pp. 186-215. Berlin: Springer-Verlag.
McGrath, C. L., Gout, J.-F., Doak, T. G., Yanagi, A. and Lynch, M. (2014). Insights into three whole-genome duplications gleaned from the *Paramecium caudatum* genome sequence. *Genetics* **197**, 1417-1428. doi:10.1534/genetics.114.163287
Merchant, S. S., Prochnik, S. E., Vallon, O., Harris, E. H., Karpowicz, S. J., Witman, G. B., Terry, A., Salamov, A., Fritz-Laylin, L. K., Maréchal-Drouard, L. et al. (2007). The *Chlamydomonas* genome reveals the evolution of key animal and plant functions. *Science* **318**, 245-250. doi:10.1126/science.1143609
Monesterolo, N. E., Santander, V. S., Campetelli, A. N., Arce, C. A., Barra, H. S. and Casale, C. H. (2008). Activation of PMCA by calmodulin or ethanol in plasma membrane vesicles from rat brain involves dissociation of the acetylated tubulin/PMCA complex. *FEBS J.* **275**, 3567-3579. doi:10.1111/j.1742-4658.2008.06502.x
Nabi, A., Yano, J., Valentine, M. S., Picariello, T. and Van Houten, J. L. (2019). SF-Assemblin genes in *Paramecium*: phylogeny and phenotypes of RNAi silencing on the ciliary-striated rootlets and surface organization. *Cilia* **8**, 2. doi:10.1186/s13630-019-0062-y
Nebl, T., Pestonjamasp, K. N., Leszyk, J. D., Crowley, J. L., Oh, S. W. and Luna, E. J. (2002). Proteomic analysis of a detergent-resistant membrane skeleton from neutrophil plasma membranes. *J. Biol. Chem.* **277**, 43399-43409. doi:10.1074/jbc.M205386200
Naitoh, Y. and Kaneko, H. (1972). Reactivated Triton-extracted models of *Paramecium*: modification of ciliary movement by calcium ions. *Science* **176**, 523-524. doi:10.1126/science.176.4034.523
Oertel, D., Schein, S. J. and Kung, C. (1977). Separation of membrane currents using a *Paramecium* mutant. *Nature* **268**, 120-124. doi:10.1038/268120a0
Padányi, R., Pászty, K., Hegedűs, L., Varga, K., Papp, B., Penniston, J. T. and Enyedi, Á. (2016). Multifaceted plasma membrane Ca^{2+} pumps: from structure to intracellular Ca^{2+} handling and cancer. *Biochim. Biophys. Acta* **1863**, 1351-1363. doi:10.1016/j.bbamcr.2015.12.011
Pani, B. and Singh, B. B. (2009). Lipid rafts/caveolae as microdomains of calcium signaling. *Cell Calcium* **45**, 625-633. doi:10.1016/j.ceca.2009.02.009
Pike, L. J. (2006). Rafts defined: a report on the Keystone symposium on lipid rafts and cell function. *J. Lipid Res.* **47**, 1597-1598. doi:10.1194/jlr.E600002-JLR200
Plattner, H. (2015). Molecular aspects of calcium signalling at the crossroads of unikont and bikont eukaryote evolution – the ciliated protozoan *Paramecium* in focus. *Cell Calcium* **57**, 174-185. doi:10.1016/j.ceca.2014.12.002
Reuter, A., Stuermer, C. and Plattner, H. (2013). Identification, localization, and functional implications ot the microdomain-forming stomatin family in the ciliated protozoa Paramecium tetraurelia. *Eukaryot. Cell* **12**, 529-544. doi:10.1128/EC.00324-12
Saidu, S. P., Weeraratne, S. D., Valentine, M., Delay, R. and Van Houten, J. L. (2009). Role of plasma membrane calcium ATPases in calcium clearance from olfactory sensory neurons. *Chem. Senses* **34**, 349-358. doi:10.1093/chemse/bjp008
Sasner, J. and Van Houten, J. (1989). Evidence for a *Paramecium* folate chemoreceptor. *Chem. Senses* **14**, 587-595. doi:10.1093/chemse/14.4.587
Satow, Y. and Kung, C. (1980). Ca-induced K^+-outward current in *Paramecium tetraurelia*. *J. Exp. Biol.* **88**, 293-304.
Sepúlveda, M. R., Berrocal-Carrillo, M., Gasset, M. and Mata, A. M. (2006). The plasma membrane Ca^{2+}-ATPase isoform 4 is localized in lipid rafts of cerebellum synaptic plasma membranes. *J. Biol. Chem.* **281**, 447-453. doi:10.1074/jbc.M506950200
Sezgin, E., Levental, I., Mayor, S. and Eggeling, C. (2017). The mystery of membrane organization: composition, regulation and roles of lipid rafts. *Nat. Rev. Mol. Cell Biol.* **18**, 361-374. doi:10.1038/nrm.2017.16
Simons, K. and Toomre, D. (2000). Lipid rafts and signal transduction. *Nat. Rev. Mol. Cell Biol.* **1**, 31-39. doi:10.1038/35036052
Strehler, E. E. (2015). Plasma membrane calcium ATPases: from generic Ca^{2+} sump pumps to versatile systems for fine-tuning cellular Ca^{2+}. *Biochem. Biophys. Res. Commun.* **460**, 26-33. doi:10.1016/j.bbrc.2015.01.121
Strehler, E. E. and Zacharias, D. A. (2001). Role of alternative splicing in generating isoform diversity among plasma membrane calcium pumps. *Physiol. Rev.* **81**, 21-50. doi:10.1152/physrev.2001.81.1.21
Tyler, K. M., Fridberg, A., Toriello, K. M., Olson, C. L., Cieslak, J. A., Hazlett, T. L. and Engman, D. M. (2009). Flagellar membrane localization via association with lipid rafts. *J. Cell Sci.* **122**, 859-866. doi:10.1242/jcs.037721
Valentine, M., Rajendran, A., Yano, J., Weeraratne, S., Beisson, J., Cohen, J., Koll, F. and Van Houten, J. (2012). *Paramecium* BBS genes are key to presence of channels in cilia. *Cilia* **1**, 16. doi:10.1186/2046-2530-1-16
Vandecaetsbeek, I., Vangheluwe, P., Raeymaekers, L., Wuytack, F. and Vanoevelen, J. (2011). The Ca^{2+} pumps of the endoplasmic reticulum and Golgi apparatus. *Cold Spring Harb. Perspect. Biol.* **3**, a004184. doi:10.1101/cshperspect.a004184
Van Houten, J. (1998). Chemosensory transduction in *Paramecium*. *Eur. J. Protistol.* **34**, 301-307. doi:10.1016/S0932-4739(98)80057-6
Wright, M. V. and Van Houten, J. L. (1990). Characterization of a putative Ca^{2+}-ATPase in the pellicles of *Paramecium tetraurelia*. *Biochim. Biophys. Acta* **1029**, 241-251. doi:10.1016/0005-2736(90)90160-P
Yano, J., Rajendran, A., Valentine, M. S., Saha, M., Ballif, B. A. and Van Houten, J. L. (2013). Proteomic analysis of the cilia membrane of *Paramecium tetraurelia*. *J. Proteomics* **78**, 113-122. doi:10.1016/j.jprot.2012.09.040
Yano, J., Valentine, M. and Van Houten, J. (2015). Novel insights into the development and function of cilia using the advantages of the *Paramecium* cell and its many cilia. *Cells* **4**, 297-314. doi:10.3390/cells4030297
Zurzolo, C. and Simons, K. (2016). Glycosylphosphatidylinositol-anchored proteins: membrane organization and transport. *Biochim. Biophys. Acta* **1858**, 632-639. doi:10.1016/j.bbamem.2015.12.018